Egypt. J. Chem. Vol. 64, No. 9, pp. 5345 - 5355 (2021)

Egyptian Journal of Chemistry

http://ejchem.journals.ekb.eg/

Role of Silver Ions in Na_2O-CaF_2-P_2O_5 Host Glass and Its Corresponding Glass-Ceramic: Searching for Antibacterial Behaviour- Supplemented by Spectral, Optical, FTIR and SEM Investigations

M. A. Ouis [a]*, A. A. Gamal [b]

[a] *Glass Research Department, National Research Centre, Cairo, Egypt.*

[b] *Chemistry of Natural and Microbial Products Department, Pharmaceutical Industries Research division, National Research Centre, Dokki, Cairo, Egypt.*

Abstract

Glasses based on the base host Na2O-CaF2-P2O5 system with increasing Ag2O as additives or loading (0.2 to 1 wt%) were prepared by melting-annealing technique. Multiple characterizations of the prepared glasses were carried out. Heat- treatment of the glasses was done through a two-step protocol to convert them to their corresponding glass-ceramics derivatives. The state of silver ions was analyzed by additional optical and FTIR spectral beside SEM measurements. Antibacterial behavior of the Ag2+ ions in the studied glasses and their glass-ceramic derivatives was conducted by their response towards two G+ve strains (Staphylococcus aureus, Bacillus cereus), one G-ve bacterial strain (Escherichia coli), one yeast (Candida albicans) and one fungi (Aspergillus niger). Optical spectra show distinct UV absorption in the undoped glass spectrum and extend to near visible with increasing Ag2O content. This distinct UV absorption is assumed to originate from unavoidable trace iron (Fe3+) impurities while the peak at 420 nm is related to nanocrystalline (Ag0)n . FTIR spectra show vibrational spectra within the mid region 400-1650 cm-1which are characteristic for phosphate (PO4) groups with some suggested (PO3F) groups. The dopant silver ions show no distinct effect on the FTIR spectra. After immersion in phosphate solution FTIR spectra of the glass-ceramic reveal the formation of hydroxyapatite layer. X-ray diffraction results indicate the formation of crystalline phosphate phases for the undoped glass-ceramic. Two silver crystalline phases are identified after addition of Ag2+ ions. SEM images confirm the formation of apatite layer with different additions of silver ion. The antibacterial analysis also indicate the promising effect of the glass-ceramics than their parent glass in the bioactivity applications.

Key words: phosphate glass; silver ion; antibacterial; optical; SEM; FTIR

1. Introduction

The last decades have been engaged by continuous and important achievements concerning the field of biomaterials and specifically, tissue engineering [1-3]. The discovery of the Hench's Bioglass causes a revolution in view and in the resultant. It was the first synthesized material to chemically and firmly bond with bone, rather than be encapsulated by fibrous tissue, and hence promoting the field of bioactive glasses and glass-ceramics.

Bioactive glasses are recognized to stimulate more bone regeneration than other bioactive ceramics, which is attributed to their easy and acceptable dissolution which efficiently producing stimulating cells at the genetic level. The result of the much favorable high responses areinitiating worldwide applications of bioactive glasses for a variety of dental and medical uses [4]. The formation of hydroxyapatite chemical layer has also been demonstrated within various borate glasses upon immersion in dilute phosphate solution and hence recommended for medical heal chronic wounds [3, 5]. Also, some

*Corresponding author e-mail: mennayy@yahoo.com
Receive Date: 23 June 2021, Revise Date: 07 July 2021, Accept Date: 12 July 2021
DOI: 10.21608/EJCHEM.2021.82197.4052

phosphate glasses are identified to give the benefit of controllable total dissolution [6] and hence have been applied for bone-repair in animals [7].

It has been accepted that many metallic ions present in the body, act as cofactors of enzymes and stimulate a chain of reactions which play important roles in a variety of diseases and metabolic disorder [2, 8]. These metallic ions include cobalt, copper, gallium, iron, manganese, silver, strontium, vanadium, zinc beside titanium [2, 8, 9]. Titanium ions in low level have been applied as promoter catalyst or initiator for the complete bonding between phosphate bioglass-ceramic and natural bone tissues [7].It is recognized that the proper antibacterial agent within a host bioglass needs to possess a broad spectrum of antibacterial activity possessing to be efficient against a broad range of G^+ and G^- bacteria, safety, minimum side effects and it should not affect the chemical and physical properties of the host carrier [10, 11].The applications of silver ions as an anti-bacterial agent in various glasses including phosphate glasses have reached favorable results [11-13]. The influence of silver ions on the bacterial properties is also visualized in borophosphate glasses [14].

The aim of the present work is to collectively characterize combined optical and FTIR spectra of some varying added or loaded Ag_2O Na_2O-CaF_2-P_2Oglasses. Besides investigating of the bioactivity and antibacterial properties of the Ag_2O-containing glasses and their glass-ceramic derivatives. The complete characterizations will be expected to throw detailed picture about the silver ions and their situation and existence form in the host soda lime fluorophosphates glass. A further supplement study includes SEM investigations of selected samples of the Ag-doped glasses and their glass-ceramics derivatives after immersion in dilute phosphate solution, searching for confirmation of their bioactivity behavior.

2. Experimental *details*

2.1. Preparation of the glasses

All glass batches were prepared from laboratory pure grade chemicals including sodium dihydrogen orthophosphate (NaH_2PO_4), calcium fluoride (CaF_2) and silver ions were introduced in the form of $AgNO_3$. The weighed batches were melted in covered porcelain crucibles at 950° C in an electric furnace (Vecstar, UK) for 60 minutes including rotating the melts at intervals to promote mixing and homogeneity. Then the melts were poured into slightly heated stainless steel molds and then immediately the prepared glassy samples were transferred to an annealing muffle regulated at 285°C. The muffle was switched off after 1 hour and left to cool to room temperature at a rate of 30°C/hour.

2.2. Optical absorption spectral measurements

The UV-visible absorption spectra were measured for undoped and Ag-doped polished samples of equal thickness (2mm±0.1 mm). The measurements were within the range 200-2500 nm using a recording spectrophotometer (type Shimadzu 3600, Japan). The measurements were also repeated to confirm the accuracy of the peaks position.

2.3. FT infrared absorption measurements

The FTIR spectra of the prepared glasses as powders were recorded at room temperature within the wavenumber range 400-4000 cm^{-1} using an IR spectrometer (type Bruker Vertex 8V, Germany). The measurements were carried out with resolution 4 cm^{-1} for the prepared glasses before and after immersion in phosphate solution.

2.4. X-ray diffraction

The crystalline phases which were separated within the glasses after thermal heat treatment process were identified by X-ray diffraction technique. The heat treated samples were ground and the fine powders were examined using a diffractometer (Philips PW 1390) adopting Ni-filter and Cu-target. Computer software (Materials studio 4.4 programs) was utilized to identify the crystalline phases formed within the heat-treated glass samples and that on surfaces after immersion in dilute phosphate solution.

2.5. Scanning electron microscope investigations (SEM)

SEM investigations were conducted on selected glass or glass-ceramic samples doped with varying Ag_2O contents at room temperature using an SEM apparatus model Philips XL30 with accelerating voltage 30 kV, magnification up to 400,000. All surfaces of the studied glasses or glass-ceramics were coated with thin layer of gold for better morphological examinations.

2.6. Biological activities of the glass samples

2.6.1. Bacterial strains

Five microorganisms selected for testing the antimicrobial activity. Two G+ve strains (Staphylococcus aureus, Bacillus cereus), one G-ve bacterial strain (Escherichia coli), one yeast (Candida albicans) and one fungus (Aspergillus niger) obtained from Department of chemistry of natural and microbial products, National Research Centre, Egypt.

2.6.2. Inoculum preparation

All used media were sterilized for inoculum preparation; nutrient agar medium used for bacteria while potato dextrose agar (PDA) medium used for fungi and yeast. The plates were incubated for 24 h at 37˚C for bacteria and 2-3 days at 30˚C for yeast and fungi.

2.6.3. Antimicrobial activity of samples by agar diffusion

Antimicrobial activity of the glass samples was carried out by agar diffusion method [15] against five indicator microorganisms. Indicator strains were Bacillus cereus, Candida albicans, Aspergillusniger, Staphylococcus aureus and Escherichia coli. Overnight culture of tested organisms [106 colony forming units/ml, (cfu/ml)] was inoculated in nutrient agar media for bacteria and potato dextrose agar for yeast and fungi, then poured immediately in sterile petri dishes. After that, samples (discs of the glass samples) were putted directly onto the surface of agar plates. The inoculated plates were incubated for 24 h at their optimum growth temperatures, and the diameter of the inhibition zone was measured in cm. The experiments were repeated two times for each microorganism strain and the results reported were the mean value [16].

3. Results

3.1. Optical absorption spectra of the studied glasses

Figure (1) illustrates the optical absorption of both the base host Na Ca fluorophosphate glass and Ag_2O-containing samples. The spectral curves reveal repetitive and parallel behavior showing strong and wide UV absorption extending from 200 to about 300 nm with two peaks at about 225 and 284 nm and with high Ag_2O-samples (0.7% and 1%) show an additional broad band centered at about 450 nm. The rest of the spectral curves are parallel with increasing the intensity with the increase of Ag_2O content.

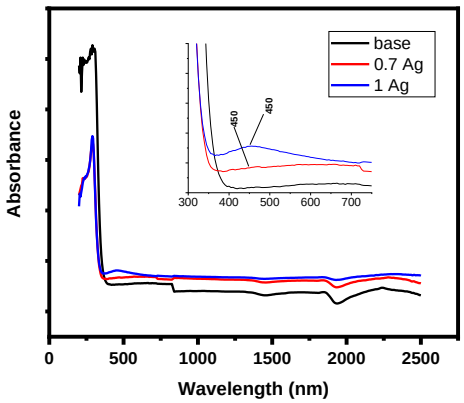

Fig (1) Optical absorption spectra of base and Ag-doped glasses

3.2. FT infrared absorption spectra of the studied glasses before immersion

Figure (2) shows the FTIR spectra of the base glass and Ag_2O containing sample before immersion in dilute phosphate solution. The IR spectral curves reveal obvious condensed vibrational bands in the mid region extended from 400 to 1650cm^{-1}. The intensities of the following absorption peaks are clearly identified with the increase of Ag_2O content: 485, 545, 707, 882, 1040, 1080, 1132, 1273, 1403, 1455, 1645 cm^{-1}.

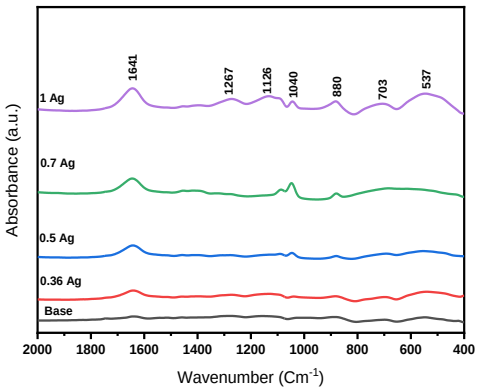

Fig (2) FTIR absorption spectra of prepared glass samples before immersion in sodium phosphate solution

3.3. FTIR spectra of the glasses after immersion in phosphate solution

Figure (3) reveals the FTIR spectra of the glasses after immersion in dilute phosphate solution for 2 weeks. The spectral curves show smoothing of the vibrational bands. Also, the intensity of the absorption bands increases with the increase of the silver ion.

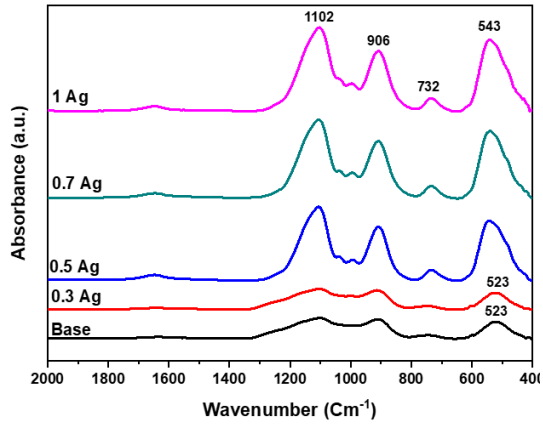

Fig (3) FTIR absorption spectra of prepared glasses after immersion in sodium phosphate solution

3.4. FTIR spectra of glass-ceramic derivatives before and after immersion in 0.25% phosphate solution

Figure (4) shows the FTIR spectra of the glass-ceramic derivatives before immersion in phosphate solution revealing quite sharp multi- bands within the range 400-1400 cm^{-1}. The following absorption peaks could be identified at: 460, 523, 580, 687, 768, 918, 997, 1109, 1164, 1267, 1308 cm^{-1} and followed by a small peak at 1640 cm^{-1}.

Figure (5) reveals the FTIR spectra of the corresponding glass-ceramic after immersion. The IR curves show the distinct appearance of connected multi peaks within the far-IR region at 423, 486, 526, 552 and 573 cm^{-1} beside the mid IR peaks at 732, 914, 950, 985, 1034, 1099, 1121, 1220, and 1250 cm^{-1}. The small peak at 1640 cm^{-1} decreases in intensity after immersion.

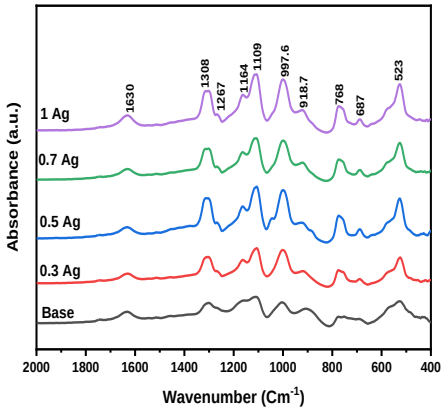

Fig (4) FTIR absorption spectra of prepared glass-ceramic before immersion in sodium phosphate solution

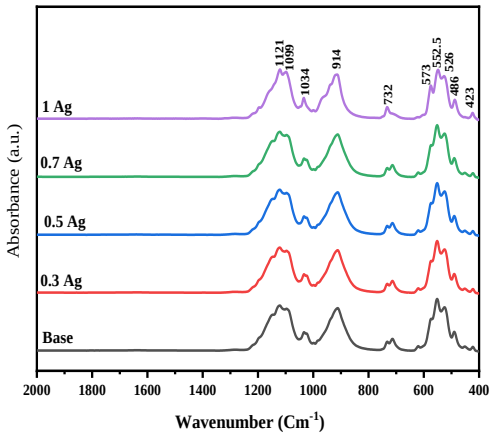

Fig (5) FTIR absorption spectra of prepared glass-ceramic samples after immersion in sodium phosphate solution

3.5. X-ray diffraction patterns data

Figures (6&7) reveal the X-ray diffraction patterns of the 3 selected glass-ceramics (base, 0.3 Ag_2O, 1 Ag_2O) before and after immersion in dilute sodium phosphate solution.

a) The X-ray data (Fig. 6) represent the formation of the following crystalline phases before immersion:
   (i) The base undoped glass-ceramic reveal the formation of three main crystalline phases of $NaPO_3$, $Ca(PO_4)_2$ and $NaPO_3F$.
   (ii) On the introduction of Ag_2O, the crystalline phases due to $NaPO_3$ and $NaPO_3F$ become sharper and more intense.
   (iii) The crystalline phase due to silver phosphate ($Ag_4P_2O_7$) can only be identified at the highest Ag_2O-doped glass-ceramic (1%).

b) The three selected glass-ceramics produce the following crystalline phases after immersion in phosphate solution: (Fig. 7)
   (i) The X-ray diffraction of the base undoped glass-ceramic reveals three distinct crystalline phases:
      - Sodium calcium fluro phosphate ($Na_5Ca_4(PO_4)4F$).
      - Sodium calcium pyrophosphate ($Na_2CaP_2O_7$).
      - Beta calcium phosphate (β-$Ca_3(PO_4)_2$).
   (ii) The two X-ray diffraction phases identified from the sample GC3 containing 0.3 % Ag_2O are as follows:
      - Silver calcium phosphate (AgCaPO4)
      - Silver phosphate (Ag5P3O10).
   (iii) X- ray diffraction of the third selected doped glass-ceramic with

the highest Ag_2O content (1%) reveals two crystalline phases namely:

- Silver calcium phosphate (AgCaPO4).
- Silver phosphate (Ag5P3O10).
- These phases are the same identified in sample GC3.

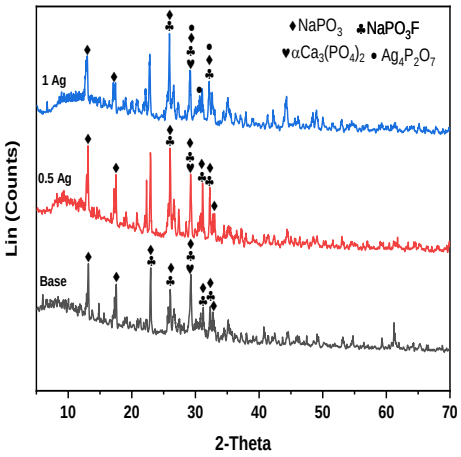

Fig(6) XRD pattern of the studied glasses before immersion in dilute phosphate solution

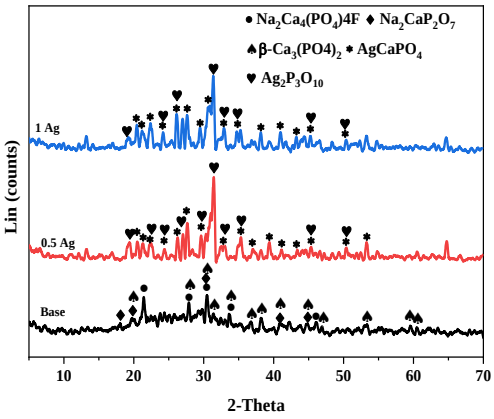

Fig (7) XRD pattern of the studied glasses after immersion in dilute phosphate solution

3.6. Scanning Electron Microscope (SEM) investigations

Figures (8-10) illustrate the SEM images of the surfaces of the three selected glass-ceramic samples (base, GC3, GC5). They show the following morphological features:

(i) The base undoped glass-ceramic shows fibrous texture and compact tissues aligned mostly in specific direction. The whole texture did not show any voids or any residual glassy phase.

(ii) The glass-ceramic sample GC3 with 0.5% Ag_2O shows a texture consisting of completely rounded or oval crystalline phase embedded on each other with minor binding remaining glassy phase.

(iii) The glass-ceramic sample No. GC5 (1%Ag_2O) shows a texture of small rounded crystalline phase connected to each other with minor remaining glassy phase.

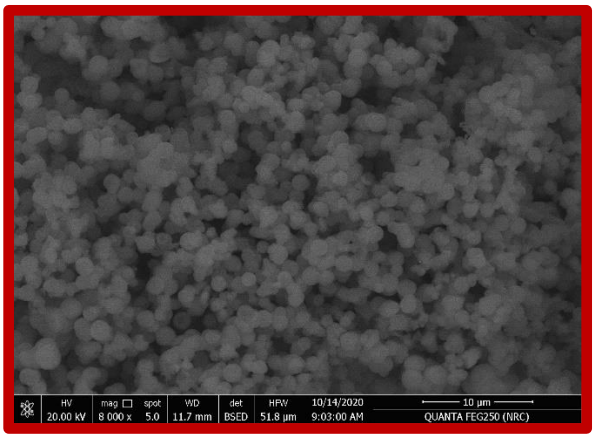

Fig (8) Scanning Electron Microscope of sample G-C5

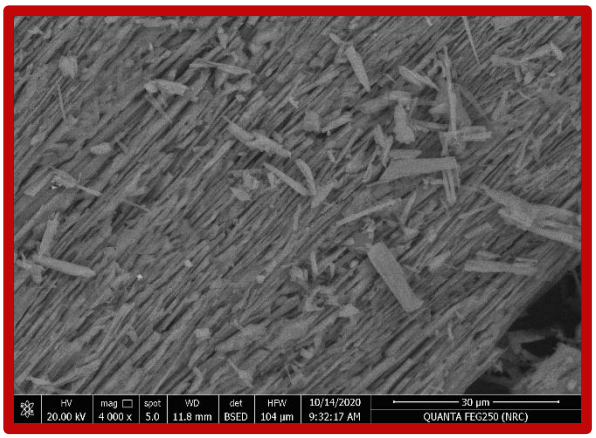

Fig (9) Scanning Electron Microscope of base glass-ceramic

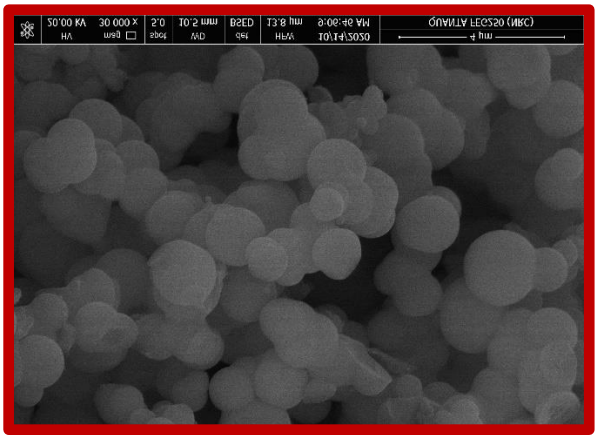

Fig (10) Scanning Electron Microscope of sample G-C 3

4. Discussion

4.1. Interpretation of the origin of the identified distinct UV-near visible absorption in the optical spectra of the studied glasses

The observed strong UV absorption with two peaks at 225 and 284 nm in the spectrum of the base host glass and extend with the spectra of Ag_2O containing glasses. This can be due to contaminated trace iron impurities present in the materials used for the preparation of the glasses. This previous assumption is in analogy with previous postulations by many earlier authors [17, 18]. The clear picture of the different UV absorption bands has been forwarded by Duffy [19]. He has assumed that traces of transition metal ions (e.g. Fe^{3+}, Cr^{6+}) exhibit distinct UV absorption even if the traces are present in the ppm level. He has referred that strong appearance is due to their charge electron transfer mechanism. Extensive studied by Ehrt and her colleagues [19-21] have agreed to the same previous assumption. Also, many publications of ElBatal and her co-authors [22-25] follow this assumption. They confirm the origin of UV absorption in various undoped phosphate, borate, and silicate glasses to trace impurities of ferric ions.

The high silver containing samples reveal as an additional broad band centered at 420 nm and this result can be explained as follows:

a. Different authors [11,13] assumed that the optical properties of silver atoms are determined in the visible region by their free electrons (Ag:[Kr] 4d10 5S1), whereas that of silver ions are determined in the ultraviolet region (Ag:[Kr]$4d^{10}S_0$).
b. Ahmed and abdallah [27] observed three absorption bands at 305, 350, and 420 nm in the spectrum of silver-containing soda lime silica glass prepared by the ion-exchange process. They attributed these three bands to be due to silver ions (Ag^+), elemental $(Ag^0)_n$, respectively.
c. Abdelghany et al. [28] assigned to the same reasoning regarding the identified visible band at 420 nm to be related to silver nanocrystallites $(Ag^0)_n$. This is obviously changing its position with the different added anion (Br^- or NO^{3-}).

We agree with the correlation between the broad visible band centered at 420 nm and the crystalline $(Ag0)_n$. The simultaneous increase of the intensity of the absorption curves with the Ag_2O content can be related to the increase of silver ions.

4.2. Interpretation of the FTIR spectra before immersion

The resultant FTIR spectra are explained and interpreted on the following parameters [29-32]:

a. FTIR spectral analysis indicates that the identified vibrational bands for the studied glasses are representing the same bands generally identified from their corresponding crystalline phosphate analogues. This confirms that the glasses reflect their structural building units by FTIR analysis in spite of their non-periodic nature. All researches accept that these vibrational bands are finger-prints of the network structural units in the studied glasses [29-32].
b. The resultant vibrational bands of the present glasses are originating from the structural units formed from their main glass-formers. The host studied glass consists of main P_2O_5 (65%) forming the extended structural PO_4 groups as essential building units beside the presence of modifier oxide Na_2O (26.3%) beside CaF_2 with (12.7%). The last CaF_2 is assumed to have the ability to act partly as glass former component as CaF_4 besides being in modifying positions. Besides, the possibility of the formation of some (PO_3F) group, cannot be neglected.
c. The detailed assignments of the identified absorption peaks can be summarized as follows [29-32]:
    (i) The vibrational peaks at 400-550 cm^{-1} are correlated with vibrations of metal cations (Na^+, Ca^{2+}) in their respective characteristic sites, together with bending vibrations of (O-P-O) and/or P=O.
    (ii) The peak at 700-750 cm^{-1} can be attributed to symmetric vibrations of P-O-P linkages.
    (iii) The peaks at 870-1035 cm^{-1} are related to asymmetric stretching vibrations of metaphosphate groups or (P-O-P) bridges.
    (iv) The peak at 1000-1110 cm^{-1} is due to asymmetric stretch of (P-O-P) linkages.
    (v) The peak at 1250-1300 cm^{-1} is related to asymmetric stretch of double bonded oxygen (P=O) vibrations.
    (vi) The peaks at 1640, 2850-3750 cm^{-1} are related to vibrations of POH, OH, water.

It is to be mentioned that the mid spectra are assumed to involve vibrations due to (PO_3F) groups.

4.3. Interpretation of the FTIR of glass-ceramic before and after immersion

The resultant FTIR spectral curves of the glass-ceramics reveal obvious numerous multi-peaks within the mid-region from 400 to 1460 cm^{-1} with sharper edges. This result is expected due to the presence of numerous microcrystalline phases with definite structures within the matrix structure of the heat treated glass-ceramics. These distinct and sharper features are more pronounced on the increase of the Ag ions. This result confirms that Ag ions are acting as efficient nucleation agent to obtain polycrystalline texture with definite lattice spacing.

Upon immersion, the IR spectra of the glass-ceramics show pronounced identification of high induced far-IR connected or splitted peaks within the range from 400 to about 700 cm^{-1}. These induced splitted far IR peaks denote the formation of hydroxyapatite or derivatives containing fluoride ions in this specific wavenumber region as have been identified by many other authors [6,7,11]. This refers that the prepared glass-ceramic of the studied system show distinct bioactivity than their parent glasses due to the possible action of silver ions initiating the ease formation of the crystalline hydroxyapatite phases.

4.4. Interpretation of the X-ray diffraction data

To interpret the crystallization behavior for the resultant crystalline phases in the studied sodium calcium fluorophosphate glass with different percents of Ag_2O, the following points are considered:

a. The tendency of crystallization of the studied glasses consisting of main P_2O_5 (65%) beside Na_2O(26.3%) and Ca_2F (12.7%) within the base host glass together with the addition of percent of Ag_2O can be assumed to proceed through proposed regimes or routes [32-41]:
   (i) It is recognized that the presence of few percent of P_2O_5 in a silicate glass matrix produces phase separation or leads to two separated phases as exemplified by the so-called Hench's Bioglass which contains 6% P_2O_5. This leads to voluminous and ease or rapid crystallization of the main phase of sodium calcium silicate ($1Na_2O.2CaO.3SiO_2$). Other reason is the presence of a double bond in the essential structural forming PO_4 tetrahedra which facilitates phase separation.
   (ii) The presence of CaF_2 in glass is assumed to initiate phase separation and readiness for crystallization because it is known as efficient nucleating agent. Brauer et al. [37] assumed that CaF_2 reduces the melting temperature of glasses and proposed the formation of CaF^+ structural unit which provides less-cross-linking than Ca^{2+} ions.
   (iii) Based on previous considerations, the resultant crystalline phases include sodium or calcium within the base undoped glass-ceramic. The appearance of the silver crystalline phase is expected to be identified at high addition or percent (1%) because silver ions are assumed to act as nucleating agent at low levels.
   (iv) The identification of two silver phases (silver calcium phosphate and silver phosphate) without any of the main phases of sodium calcium fluorophosphates or sodium calcium phosphate after immersion in phosphate solution, can be attributed to the dissolution of the two mentioned phosphate phases while the two silver phases remain undissolved and easily identified by X-ray diffraction analysis.

4.5. Interpretation of the SEM data

The interpretation of the SEM images identified in Figures (8-10) can be summarized as follows:

(i) The complete longitudinal fibrous texture of the base undoped glass-ceramic is expected from the collected different micro-crystalline phosphate phases originating in accordance with the main glass constituents (namely phosphate of calcium and sodium). It is obvious that the crystalline phases are precipitated or formed through suggested phase separation and followed by voluminous crystallization with the aid of P_2O_5 and CaF_2 as nucleators.
(ii) The two Ag_2O doped glass-ceramics reveal rounded or circular shaped microcrystals which is larger in size in the low percent glass-ceramic (0.5% Ag_2O)but show smaller size in the highest Ag_2O 1% sample. This behavior can be correlated with the presence of silver ions as a promoter or catalyst which upon increasing produce small round-shaped microcrystals all over the entire texture.

4.6. Antimicrobial behaviour results

The antimicrobial effects of the glass under investigation on different bacterial strains are illustrated in [Table (1), Fig. (11)]. The glass samples

showed promising antimicrobial activity against all the tested microorganisms except the base glass-ceramic sample. For 0.3 Ag glass, the highest growth inhibition can be observed with E. coli (4.50 cm) and the lowest is observed with Candida albicans (3.30 cm). This means that C. albicans reveals greater resistance to the current glass sample. The lowest antimicrobial activity is found at 0.7 Ag against staphylococcus aureus (2.50 cm). It has been observed that antimicrobial activities against B. cereus, S. aureus, E. coli, C. albicans and A. niger bacteria decrease by increasing the concentration of Ag and this result can be explained to be due to the possible toxic effect of increasing silver ions.

Table (1): The antimicrobial activity of the prepared glass samples on different microbial strains

Glass samples	Inhibition zone of microbial growth (Cm)				
	Microorganisms				
	Bacillus cereus	Staphylococcus aureus	Candida albicans	Aspergillus niger	E. coli
Base	---	---	---	---	---
0.3 Ag	4.20	3.50	3.30	3.80	4.50
0.5 Ag	3.50	3.00	3.10	3.20	3.10
0.7 Ag	3.10	2.50	2.90	2.70	3.00
1.0 Ag	2.90	2.60	3.00	2.80	2.70

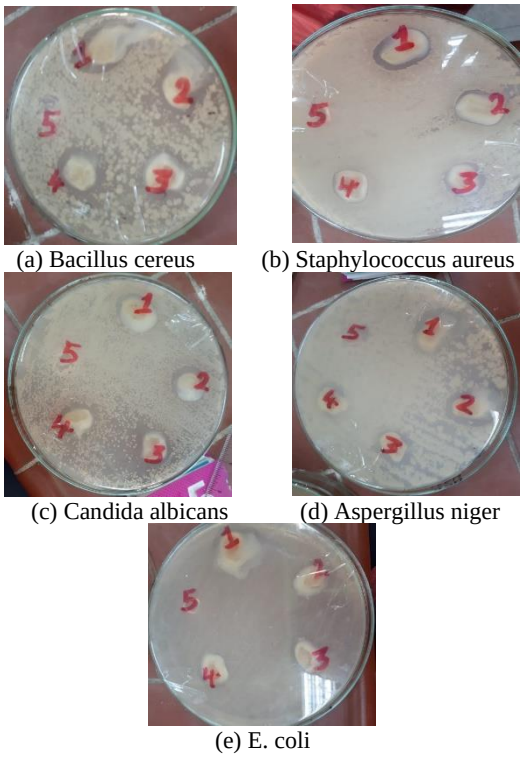

(a) Bacillus cereus (b) Staphylococcus aureus (c) Candida albicans (d) Aspergillus niger (e) E. coli

Fig (11) Petri dishes of antimicrobial activity of glass samples against (a) Bacillus cereus (b) Staphylococcus aureus (c) Candida albicans (d) Aspergillus niger (e) E. coli

From the first investigation, it was found that B. cereus was the most sensitive organism to the prepared glass samples, so it was chosen for the following experiment against the glass ceramic samples. In contrary with glass samples. The results illustrated in Table (2) and Fig. (12) show that all glass ceramic samples exhibit promising antimicrobial activity against all tested microorganisms. The 1.00 Ag glass ceramic is identified to be the most potent antimicrobial agent against B. cereus.

Table (2): The antimicrobial activity of the prepared glass ceramic samples on *Bacillus cereus*

Glass ceramic	Inhibition zone of microbial growth (Cm)
	Bacillus cereus
Base	**2.50**
0.3 Ag	**2.50**
0.5 Ag	**3.00**
0.7 Ag	**2.50**
1.0 Ag	**3.30**

(a) Front (b) Back

Fig. (12) Petri dish of antimicrobial activity of glass ceramic samples against Bacillus cereus (a) Front of Petri dish (b) Back of the Petri dish

4.7. Suggested mechanism of antibacterial activities of the glass and related glass-ceramic

Before discussing the mechanism of antibacterial activities, the state of silver ions in the host Na_2O-CaF_2-P_2O_5 glass can be advanced in the following points:

(i) It is known that silver ions can exist in glass in three possible states, Ag^0, Ag^+ and Ag^{2+} and this can be controlled by referring to the glass type and its constituents and melting condition including temperature and atmosphere of preparation. The host phosphate glass is known to be able to dissolve high percent of transition metal ions (e.g. V^{5+}, Fe^{3+})and the silver ions is added in low percent to avoid toxicity. The glass consists of major P_2O_5 65% and hence is acidic in nature and phosphate glasses are known to initiate lower valence of TM ions. On the other hand, the introduction of silver ions as $AgNO_3$ beside the presence of Na_2O (26.3%) promotes the presence of silver ions in two possible valences (Ag^0 + Ag^+). The optical spectra refer to the appearance of distinct UV absorption beside the resolution of the plasmon

peak around 420 nm due to silver nano-crystallites $(Ag^0)n$ together with the sharing of electronic transitions involving Ag^+ ions ($4d^0$ $4d^0$ $5S^1$).

(ii) It is equally important to refer that the acidity or alkalinity of the surrounding medium affects the growth of bacteria and fungi. Most bacteria survive near neutral condition within the PH range 6.7 and 7.5. Thus, the change in the PH during the immersion of the host phosphate glass with acidic character could explain the bacterial growth inhibition produced by the ease of such glass.

The silver containing glasses upon immersion in aqueous medium or in the presence of moisture, these glasses gradually dissolve and during this dissolution, the silver ions (the antibacterial active agent) are releases in to the medium and inhibit the growth of bacteria.

Several mechanisms for the antibacterial action of silver ions are introduced by several authors: [41-45]

a. Kim el al. [42] proposed that Ag^+ ions interfered with the metabolism of the micro-organism, thus inhibiting its growth.
b. Feng et al [43] suggested that the antibacterial mechanism was due to DNA not being able to replicate, and proteins becoming inactivated after contact with Ag^+ ion.
c. Chappell and Greville [44] assumed that low level of Ag^+ ions collapsed the proton motive force on the membrane of bacteria.
d. Dibrov et al. [45] argued that low concentration of Ag^+ ions produced a massive proton leakage through the bacterial membrane, resulting finally to cell death.

The biochemical metabolic mechanism of glass samples for inhibition of growth of various pathogens including Escherichia coli, Staphylococcus aureus, Bacillus cereus, Candida albicans and Aspergillusniger is explained by many mechanisms one of them is chemical capability of natural metabolites to bind chemically with nucleic acids represented by DNA and RNA leading to decrease or inhibit the biochemical and physiological functions of these samples in the pathogenic bacteria cell [16,46] .Also the hydroxyl group(s) abundant have chemical ability for destruction of the wall and membrane belonging to pathogens cell leading to change in the tertiary structure of proteins existing in the cell of pathogenic bacteria. Some studies proved the high ability of silver ions (heavy metals) to distract the primary metabolism of lipids, carbohydrates and proteins present in the living cell of pathogenic bacteria leading to consumption of biochemical energy of these pathogens. Also the heavy metals are capable for decrease and/or finish the biochemical roles of various enzymes of microorganisms including pathogenic bacteria causing to inflammatory and infections in human body [47-48].

5. Conclusions

Glasses of base and Ag_2O containing within the host Na_2O-CaF_2-P_2O_5 system were prepared and characterized. Optical spectra of the glasses reveal distinct UV absorption due to contaminated unavoidable iron impurities. In the Ag_2O- doped samples the UV spectra exhibit extra extension and appearance of near visible band at 420-450 nm due to suggested nanocrystalline $(Ag°)_n$ FTIR spectra of the glasses and their corresponding glass-ceramics before immersion reveal characteristic peaks due to phosphate groups (PO_4) with some sharing of (PO_3F) vibrations within the mid region. The glass-ceramic samples exhibit sharper peaks due to expected micro-crystallinity. FTIR after immersion reveal lower intensities of the vibrational peaks due to dissolution process of the main phosphate phases in the immersion solution. The IR spectra of glass-ceramics after immersion show the appearance of distinct far-IR peaks due to the assumption of the formation of hydroxyl-fluoroapatite. This behavior indicates that the glass-ceramic derivatives reveal distinct bioactivity than their parent glass. The antibacterial data indicate encouraging results specifically for glass-ceramic samples.

6. Conflicts of interest

We confirm that there are no known conflicts of interest associated with this publication and there has been no significant financial support for this work that could have influenced its outcome.

7. Acknowledgments

We wish to acknowledge Glass Research Dept., and Chemistry of Natural and Microbial Products Department, National Research Centre.

8. References

[1] M.N. Rahman, D.E. Day, B.S. Bal, Q. Fu, S.B. Jung, L.F. Bonewald, A.P. Tomasia, Bioactive glass in tissue engineering, Acta Biomater. 7 (2011) 2355.
[2] V. Mourino, J.P. Cattalini, A.R. Boccaccini, Metallic ions as therapeutic agents is tissue engineering scaffolds: an overview of their biological applications and strategies for new developments, J. R. Soc. Interface 9 (2012) 401.
[3] J.R. Jones, D.S. Brauer, L. Hupa, D.C. Greenspan, Bioglass and Bioactive glasses and their impact on healthcare, Intern. J. Appl. Glass Sci. 7 (2016) 423.
[4] L.L. Hench, Bioglass: 10 milestones from concept to commerce, J. Non-Cryst. Solids 432 (2016) 2.
[5] S.B. Jung, D.E. Day, T. Day, W. Stoecker, P. Taylor, Treatment of non-Heching Diabetic Vanous Stasis Ulters with Bioactive Glasses and Glass-Ceramics, Wound Repair Regen. 19 (2011) A30.

[6] E.A. Abou Neel, D.M. Pickup, S.P. Valappil, R.J. Newport, J.C. Knowles, Bioactive Functional Materials A Prospective on Phosphate-Based Glasses, J. Mater. Chem. 19 (2009) 690.
[7] A.S. Monem, H.A. ElBatal, E. Khalil, M.A. Azooz, Y.M. Hamdy, In vivo behavior of bioactive phosphate glass-ceramics from the system P_2O_5-Na_2O-CaO containing TiO_2, J. Mater. Sci. Mater. Med. 19 (2008) 1097.
[8] V. Maurino, A. Boccaccini, Bone tissue engineering therapeutics Controlled drug delivery in three-dimensional scaffolds, J. R. Soc. Interface 7 (2010) 209.
[10] J.R. Uzarzki, Investigation of Bacteria visibility on surfaces using functional Alkanethiol self Assembed Monolayers, M.Sc. Thesis, USA (2006).
[11] A.A. Ahmed, A.A. Ali, D.A.R. Mahmoud, A.M. El-Fiqi, Study on the Preparation and Properties of Silver-Doped Phosphate Antibacterial Glasses (Part I), Solid State Sci. 13 (2011) 981.
[12] M. Bellantone, H.D. Williams, L.L. Hench, Bradd-Spectrum bacterioidal activity of Ag_2O-doped bioactive glass, Antimicrob. Agents Chemother. 46 (2002) 1940.
[13] A. Mullgan, M. Wilson, J.C. Knowles, Effect of increasing silver content in phosphate based glasses on biofilms of *streptococcus sanguis*, J. Biomed. Mater. Res. Part A 67 (2003) 401.
[14] K. Magyari, R. Stefan, D.C. Vodnar, A. Vulpoi, L. Baia, The silver influence on the structure and antibacterial properties of the bioactive B_2O_3-30 Na_2O-60 P_2O_5 glass, J. Non-Cryst. Solids 402 (2014) 182.
[15] V. Mishra, D.N. Prasad, Application of in vitro methods for selection of *Lactobacillus casei* strains as potential probiotics, Int. J. Food Microbial. 103 (2005) 109.
[16] M.A. Sherief, G.T. El-Bassyouni, A.A. Gamal, M.A. Esawy, Modification of diatom using silver nanoparticles to improve antimicrobial activity, Mater. Today: Proceed. 43 (2021) 3369.
[17] J.R. Sigel, R.J. Ginther, The effect of iron on the ultraviolet absorption of high purity soda-silica glass, Glass Technol. 9 (1968) 66.
[18] L. Cook, K.H. Mader, Ultraviolet Transmission Characteristics of a Fluorophosphate Laser Glass, J. Amer. Ceram. Soc. 597 (1982) 801.
[19] J.A. Duffy, Charge transfer spectra of metal ions in glass, Phys. Chem. Glasses 38 (1997) 289.
[20] D. Möncke, D. Ehrt, Irradiation induced defects in glasses resulting in the photoionization of polyvalent dopants, Opt. Mater. 25 (2004) 425.
[21] D. Ehrt, Glass chemical research in the spirit of Otto Schott, Phys. Chem. Glasses: Eur. J. Glass Sci. Technol. (B) 56 (2015) 217.
[22] F.H. ElBatal, S.M. AboNaf, Spectroscopic studies of gamma-irradiated transition metals-doped soda lime phosphate glass, Indian J. Pure & Appl. Phys. 43 (2005) 679.
[23] F.H. ElBatal, M.A. Marzouk, A.M. Abdelghany, Gamma rays interaction with bismuth borate glasses doped by transition metal ions, J. Mater. Sci. 46 (2011) 5140.
[24] M.A. Marzouk, H.A. ElBatal, R.L. Elwan, Effect of MoO_3, MnO_2 or mixed dopants on the spectral properties and crystallization behavior of sodium phosphate glasses containing either MgO or MgF_2, Appl. Phys. (A) 125 (2019) 1383.
[25] R.H. Doremus, Optical properties of small silver particles, J. Chem. Phys. 42 (1965) 411.
[26] Chakraborty, P., Metal nanoclusters in glasses as non-linear photonic materials, J. Mater. Sci. 33 (1998) 223.
[27] A.A. Ahmed, E.W. Abdallah, Origin of Absorption Bands Observed in the Spectra of Silver Ion Exchanged Soda–Lime–Silica Glass, J. Amer. Ceram. Soc. 78 (1995) 2777.
[28] A. Abdelghany, H.A. ElBatal, F.H. ElBatal,Spectral studies of silver ions in barium borate glass and effects of gamma irradiation, Middle East J. Appl. Sci. 5 (2015) 1.
[29] J. Wong, C.A. Angell, The glass–liquid transition of hyperquenched water, New York (1976).
[30] A. Abel-kader, A.A. Higazy, M.M. ElKholy, Compositional dependence of infrared absorption spectra studies for TeO_2-P_2O_5 and TeO_2-P_2O_5-Bi_2O_3 glasses, J. Mater. Sci. Mater. Electr. 2 (1991) 157.
[31] Y.M. Mostaffa, K. El-Egili, Infrared spectra of sodium phosphate glasses, J. Non-Cryst. Solids 240 (1998) 144.
[32] M.A. Marzouk, Y.M. Hamdy, H.A. ElBatal, Photoluminescence and spectral performance of manganese ions in zinc phosphate and barium phosphate host glasses, J. Non-Cryst. Solids 458 (2017) 1.
[33] P.W. McMillan, Physics in glass technology, Phys. Educ. 14 (1979) 441.
[34] W. Höland, W. Vogel, K. Naumann, J. Gumme, Interface reactions between machinable bioactive glass-ceramics and bone, J. Biomed. Mater. Res. 19 (1985) 303.
[35] W. Höland, phase formation and properties of dental glass-ceramics in the SiO_2-AL_2O_3-K_2O-CaO-P_2O_5 AND SiO_2-Li_2O-ZrO_2-P_2O_5 SYSTEMS, phosph. res. bull. 6 (1996) 111.
[36] W. Höland, G.H. Beall, Glass- Ceramic Technology, 3rd ed. The Amer. Ceram. Soc. 36 (2002) 215.
[37] P. Hudon, D.R. Baker, The nature of phase separation in binary oxide melts and glasses. II. Selective solution mechanism,J. Non-Cryst. Solids 303 (2002) 346.
[38] C. Rüssel, D. Tauch, R. Garkova, S. Woltz, G. Volkesh, Phase separation and crystallisation in borate glasses, Phys. Chem. Glasses, Eur. Glass. Sci. Technol (B), 47 (2006) 397.
[39] D.S. Brauer, RG., Hill, M.D.O. Donnell., Crystallisation of fluoride-containing bioactive glasses, Phys. Chem. Glasses: Eur. J. Glass Sci. & Technol. (B) 53 (2012) 27.
[40] F.H. ElBatal, M.A. Ouis, H.A. ElBatal, Comparative studies on the bioactivity of some borate glasses and glass–ceramics from the two systems: Na_2O–CaO–B_2O_3 and NaF–CaF_2–B_2O_3, Ceram. Intern. 42 (2016) 8247.
[41] H.A. ElBatal, A.A. ElKheshen, M.A. Marzouk, N.A. Ghoneim, F.H. ElBatal, M.A. Ouis, A.M. Fayad, A.M. Abdelghany, In vitro bioactivity of silicophosphate glasses doped with ZnO, SrO or CuO, J. Theor. Appl. Phys. 14 (2020) 159.
[42] T.N. Kim, Q.L. Feng, J.Q. Kim, I. Wu, H. Wang, G.C. Chem, F.Z. Cui, Antimicrobial effects of metal ions

(Ag^{+}, Cu^{2+}, Zn^{2+}) in hydroxyapatite, J. Mater. Sci. Mater. Med. 9 (1998) 129.

[43] Q.L. Feng, J. Wu, G.Q. Chen, F.Z. Cui, T.N. Kim, J.O. Kim, A mechanistic study of the antibacterial effect of silver ions on *Escherichia coli* and *Staphylococcus aureus*, J. Biomed. Mater. Res. 52 (2000) 662.

[44] J.B. Chappell, G.D. Greville, Effect of Silver Ions on Mitochondrial Adenosine Triphosphatase Nature, 174 (1954) 930.

[45] P. Dibrov, J. Dzioba, K.K. Gosink, C. Hase, Chemiosmotic Mechanism of Antimicrobial Activity of Ag^{+} in Vibrio cholera, Antimicrob. Agents Chemother. 8 (2002) 2668.

[46] H. Jayasuriya**,** M.K. Napharan**,** R.I. Geahlen**,** J.L. Mclanghlin**,** C.J. Chang**,** Emodin, a protein tyrosine kinase inhibitor from *Polygonum cuspidatum***.** J. Nat. Prod. 55 (1992) 696.

[47] M. Ghasemian, S. Owlia, M.B. Owila., Review of anti-inflammatory herbal medicines, Adv. In pharmacol. Sci. 11 (2016) 1.

[48] M.S. Hanafy, W.M. Desoky, E.M. Hussein, N.H. ElShaer, M. Gomaa, A.A. Gamal, M.A. Esawy, O.W. Guirguis, Biological applications study of bio-nanocomposites based on chitosan/TiO_2 nanoparticles polymeric films modified by oleic acid, J. Biomed. Mater. Res. 109 (2021) 232.